

Model-Based Observers for Tire/Road Contact Friction Prediction

Carlos Canudas de Wit¹, Roberto Horowitz² and P. Tsiotras³

¹Laboratoire d'Automatique de Grenoble, UMR CNRS 5528
ENSIEG-INPG, ST. Martin d'Hères, France.

²Department of Mechanical Engineering, University of California
Berkeley, CA 94720-1740, U.S.A.

³Georgia Institute of Technology, School of Aerospace Eng. Atlanta,
Georgia 30332-0150, U.S.A.

1 Introduction

This contribution is devoted to the problem of tire-road friction estimation. The need for such type of studies, stems from the difficulty of direct sensing of tire forces, slip, slip angles and other external factors. Observer algorithms are, in this context, a low cost alternative for sensors. Tire forces information is relevant to problems like: optimization of Anti-lock brake systems (ABS), traction system, diagnostic of the road friction conditions, etc.

Literature for tire/road friction estimation is numerous. Bakker *et al* [1] and Burckhardt [4] describe two analytical models for tire/road behavior that are intensively used by researchers in the field. In these two models the coefficient of friction, μ , or more precisely, the normalized friction force, i.e.

$$\mu = \frac{F}{F_n} = \frac{\text{Friction force}}{\text{Normal force}}$$

is mainly determined based on the wheel slip s and some other parameters like speed and normal load. Fig. 1 shows two curves, obtained from Harned *et al* [9], that represent typical μ versus s behavior.

It is current practice to name the ratio between the friction and the normal forces, μ , as being the "coefficient" of friction. Under constant normal force conditions, μ , is a constant if and only if the Coulomb model is used to describe friction. Nevertheless, the Coulomb model is too simplistic to suitable represent forces between the rubber tire and the road, which are dominated by the elasto-plastic force/displacement characteristics. Therefore, to consider μ as a constant is a pure idealistic view. μ should thus

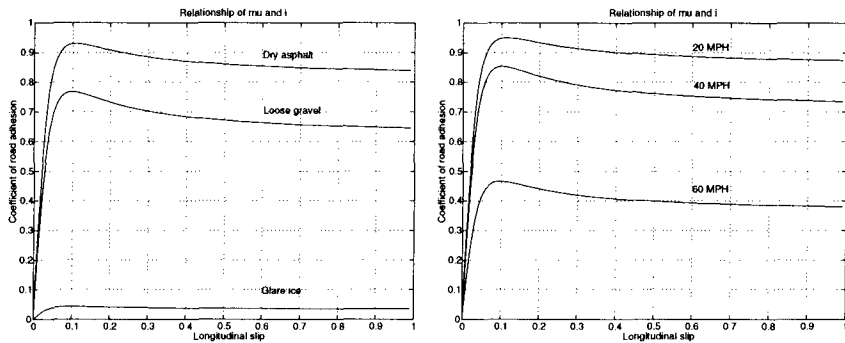


FIGURE 1. a) Variations between coefficient of road adhesion μ and longitudinal slip s for different road surface conditions (left). b) Variations between coefficient of road adhesion μ and longitudinal slip s for different vehicle velocities (right).

be viewed more as the ratio between friction and normal forces (i.e. the normalized force), which is indeed a (static or dynamic) function of the system state variables.

The expression given by Bakker *et al* [1], and Pacejka and Sharp [14], also known as “magic formula” is derived heuristically from experimental data to produce a good fit. It provides the tire/road coefficient of friction μ as a function of the slip s . The expression in Burckhardt [4] is derived with a similar methodology. The final map expresses μ as a function of s , the vehicle velocity, v and the normal load on the tire F_n .

Kiencke [10] presents a procedure for real-time estimation of μ . A simplification to the analytical model by Burckhardt [4] is introduced in such a way that the relation between μ and s is linear in the parameters. Kiencke [10] uses a two stages identification algorithm. In the first stage, the value of μ is estimated. This estimate of μ is used in the second stage to obtain the parameters for the simplified μ versus s curve.

The paper by Gustafsson [8] derives an scheme to identify different classes of roads. He assumes that by combining the slip and the initial slope of the μ versus s curve it is possible to distinguish between different road surfaces. The author tests for asphalt, wet asphalt, snow and ice and identifies the actual value of the slope with a Kalman filter and a least square algorithm.

Ray [16] estimates μ based on a different approach. Instead of using the slip information to derive a characteristic curve, Ray [16] estimates the forces on the tires with an extended Kalman filter. Using a tire model introduced by Szostak *et al* [17], that expresses the tire forces as a function of μ , the author tries this model for different values of μ . A Bayesian approach is used to determine the value of μ that is most likely to produce the forces estimated with the extended Kalman filter.

The works of Kiencke [10], Gustafsson [8], and Ray [16] do not consider any velocity dependence in the derivation of μ , as suggested by Burckhardt

[4] and Harned *et al* [9]. An attempt to consider the velocity dependence for ABS control is presented in Liu and Sun [13]. The authors assume the tire/road characteristics to be known. Due to the limitations in the available data, the authors are not able to compare their algorithm with other methods.

There are other works related to the on line identification of the tire/road friction, as for example Lee and Tomizuka [12], and Yi and Jeong [18]. However, in these papers only the instantaneous coefficient of friction is identified.

The coefficient of tire/road friction, or coefficient of road adhesion, μ is mainly a function of the longitudinal slip, the velocity of the vehicle and the normal load.

The estimators proposed in the literature depends very much on the type of used models, and verification of the hypothesis used for the model derivation. As shown by the figures above, the relation of the curves $\mu-s$, depends very much on system operating conditions, such as the vehicle velocity. It is clear that parameters describing a curve like the one in Fig .1-(a), will not be invariant, as shown in Fig .1-(b). It is thus interesting to introduce models described by parameters that are more likely to be invariant and have physical significance. Theory never exactly matches reality, but some times closely resembles it.

To achieve this goal, we propose in this paper to use a dynamical tire/road friction model, together with a nonlinear observer specifically designed for this application. This paper is organized as follows: The next section reviews some of the existing tire/road friction models, and also introduces lumped and distributed dynamic representations. In Section 3 we set-up the observation problem, using the particular case of a one-wheel system with lumped contact friction. Inspired from previous works by Canudas-de-Wit and Lischinsky [6] on adaptive friction estimation and compensation, Section 4 presents a general framework for the design of nonlinear observers for the on-line estimation of the road conditions. In Section 5 we apply this design to the case study case set in Section 3. Finally, Section 6 presents simulation results.

2 Tire-road Friction Models

This section reviews some friction models that can be used for the study of the on-line identification of the friction force (or coefficient, if we consider normalized force). We first present the some of the pseudo steady-state models proposed in the literature, then we discuss some alternative dynamic (lumped and a distributed) models.

The sep up for this study is the simple case of an one-wheel model with tire-road contact friction, shown schematically in Fig. 2. In this study we

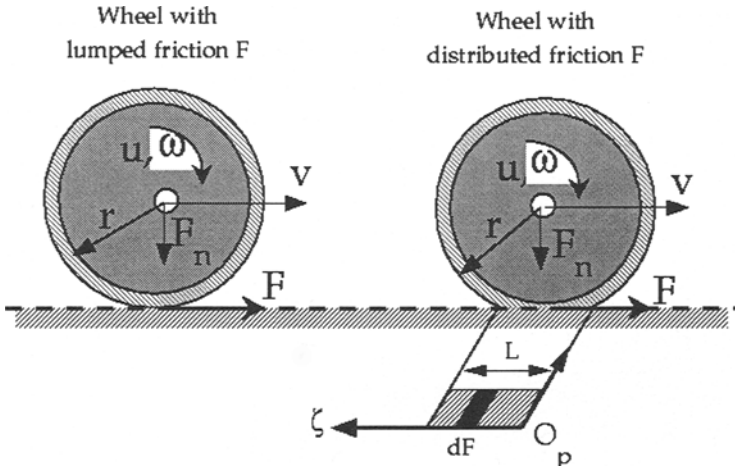


FIGURE 2. One-wheel system with: lumped friction (left), distributed friction (right)

will thus consider a system of the form

$$m\dot{v} = F \quad (2.1)$$

$$J\dot{\omega} = -rF + u_\tau - \sigma_\omega\omega, \quad (2.2)$$

where:

m – wheel mass,

J – wheel inertia,

r – wheel radius,

v – linear velocity,

ω – angular velocity,

u_τ – braking/driving torque,

F – tire/road friction force.

Therefore, only longitudinal motion (longitudinal slip) will be considered.

2.1 Pseudo-Steady State Models

This type of models are currently used in the literature. They are defined as one-to-one (memory less) maps between the friction F , and the longitudinal slip rate s , defined as:

$$s = \begin{cases} \frac{v-r\omega}{v} & \text{if } v > r\omega, v \neq 0 & \text{braking} \\ \frac{r\omega-v}{r\omega} & \text{if } v < r\omega, \omega \neq 0 & \text{driving} \end{cases} \quad (2.3)$$

The slip rate results from the reduction of the effective circumference of the tire (consequence of the tread deformation due to the elasticity of the tire rubber), which implies that the ground velocity will not be equal to $v = r\omega$. The slip rate is defined in the interval $[0, 1]$. When $s = 0$ there is no sliding (pure rolling), whereas $s = 1$ indicates full sliding.

In opposition to steady-state friction models, the pseudo steady-state (PSS) models aim at describing the shapes shown in Fig.1 via static maps $F(s)$, mapping s to F , and not as a steady-state relation between contact relative velocity and friction forces. They are named pseudo steady-state because some of these models depend on the vehicle velocity v , i.e. $F(s, v)$. The models also depends on the operating conditions, although they are only valid under steady-state conditions.

One of the most well known models of this type is Pacejka's model (see, Pacejka and Sharp [14]), also known by the name of "magic formula". This model has been shown to suitably match experimental data, obtained under particular conditions of constant linear and angular velocity. The Pacejka model has the form

$$F(s) = c_1 \sin(c_2 \arctan(c_3 s - c_4(c_3 s - \arctan(c_3 s)))) ,$$

where the $c'_i s$ are the parameters characterizing this model. The parameters can be identified by matching experimental data, as shown in Bakker *et al* [1].

The model proposed by Burckhardt [4] for the tire/road friction characteristics is of the form

$$F(s, v) = (c_1(1 - e^{-c_2 s}) - c_3 s) e^{-c_4 v} , \quad (2.4)$$

where c_1, \dots, c_4 are constants. The normal load at the tire is kept constant in this model. Note also the velocity dependency of this model, seeking to match variations like the one shown in Fig. 1-(b).

Kiencke and Daiss [11] neglect the velocity dependent term in Eq. (2.4) and approximate the curve by

$$F(s) = K_s \frac{s}{c_1 s^2 + c_2 s + 1} , \quad (2.5)$$

where K_s is the slope of the $F(s)$ versus s curve when $s = 0$ and c_1 and c_2 are properly chosen parameters. Notice that Eq. (2.5) is only dependent on the slip s . The value of K_s is assumed to be known. Kiencke and Daiss [11] choose a fixed value of about 30° for it.

Alternative, Burckhardt [3] proposes a simpler three parameters model,

$$F(s) = c_1(1 - e^{-c_2 s}) - c_3 s .$$

Since these models are highly nonlinear in the unknown parameters, they are not well adapted to be used for on-line identification. For this reason, simplified models like

$$F(s) = c_1 \sqrt{s} - c_2 s$$

are used in connection with a linear recursive identification algorithms, has been proposed in the literature.

A part from the nonlinearity in the unknown parameters, the major limitation of this models seems to stem from the fact that the unknown parameters are not really invariant, they may strongly depend on the tire characteristics (such as compound, tread type, tread depth, inflation pressure, temperature), on the road conditions (such as type of surface, texture, drainage, capacity, temperature, lubricant, i.e. water or snow), and on the vehicle operational conditions (velocity, load), see Pasterkamp and Pacejka [15].

As an alternative to the pseudo static models that depend instantaneously only on s (memory-less models), dynamic models based on the preliminary studies on dynamic friction models of Dahl [7], can be adapted to suitably describe the road-tire contact friction. The Dahl's models leads to a friction displacement relation that bears much resemblance with stress-strain relations proposed in classical solid mechanics.

A potential advantage of such models is their ability to describe some of the physical phenomena found in road/tire friction (such as: hysteresis loops, pre-sliding displacement, etc), as well as their dependance on parameters that may have physical meaning. Although the parameters of such models, may also depend on some of the factors mentioned above, other parameters may be more like to be invariant, or be more directly related with the phenomena to be observed, like for instance the change on the road characteristics (i.e. dry wet, etc.). Dynamic models can be formulated as a lumped or distributed models, as shown in Fig. 2. This distinction will be discussed next.

2.2 Lumped Dynamic Models

A lumped friction model assumes punctual tire-road friction contact. An example of such a model can be derived from the LuGre model (see Canudas *et al*, [5]). This model differs from the one in [5] in the way that the function $g(v)$ is defined. Here we propose to use the term $e^{-|v_r/v_s|^{1/2}}$ instead the term $e^{-(v_r/v_s)^2}$ as in the LuGre model in order to better match the pseudo-stationary characteristic of this model (map $s \mapsto F(s)$) with the shape of the Pacejka's model, as it will be shown later.

The model of Canudas *et al*, [5] is written:

$$\dot{z} = v_r - \frac{\sigma_0 |v_r|}{g(v_r)} z \quad (2.6)$$

$$F = (\sigma_0 z + \sigma_1 \dot{z} + \sigma_2 v_r) F_n \quad (2.7)$$

with,

$$g(v_r) = \mu_C + (\mu_S - \mu_C) e^{-|v_r/v_s|^{1/2}}$$

where,

σ_0 – rubber longitudinal lumped stiffness,

σ_1 – rubber longitudinal lumped damping,

σ_2 – viscous relative damping,

μ_C – normalized Coulomb friction,

μ_S – normalized Static friction, $\mu_C \leq \mu_S, \in [0, 1]$,

v_S – Stribeck relative velocity,

F_n – normal force,

v_r – relative velocity = $(r\omega - v)$,

z – internal friction state.

Remark: This model, has the following important properties:

- (i) if $|z(0)| < \mu_S/\sigma_0$, thus $|z(t)| < \mu_S/\sigma_0, \forall t \geq 0$,
- (ii) $\infty > \mu_S \geq g(v_r) \geq \mu_C > 0, \forall v_r$
- (iii) the right hand side of (2.6) is Lipschitz (globally if v_r is assumed bounded, and locally if not).

In particular Property (i) ensures that the internal friction states are bounded and that its upper bound is given by the static friction parameter (Property (ii)). Property (iii), provides existence and uniqueness of a solution to (2.6).

2.3 Distributed Dynamic Models

Distributed models assume the existence of an area of contact (or patch) between the tire and the road, as shown in Fig. 2. This patch represent the projection of the part of the tire that is in contact with the road. The contact patch is associated to the frame O_p , with ζ as the axis coordinate. The patch length is L .

Distributed dynamical models, as well as their relation with the pseudo-static models, has been studied previously in works of Bliman *et al* [2]. They propose second order rate independent model (similar to the Dahl ones), and have shown that, under constant v and ω , there exist a choice of parameters that closely match a curve similar to the one characterizing the magic formula.

Similar results can be obtained by using a model based in the first-order LuGre friction model, i.e.

$$\frac{d\delta z}{dt}(\zeta, t) = v_r - \frac{\sigma_0 |v_r|}{Lg(v_r)} \delta z \quad (2.8)$$

$$F = \int_0^L dF(\zeta, t) d\zeta, \quad (2.9)$$

with $g(v_r)$ defined as before and

$$dF = \left(\frac{\sigma_0}{L} \delta z + \sigma_1 \delta \dot{z} + \sigma_2 v_r \right) dF_n,$$

where,

σ_0/L – rubber longitudinal distributed stiffness per length,

dF – differential friction force,

dF_n – distributed normal force [F_n/L],

v_r – relative velocity = $(r\omega - v)$,

δz – differential internal friction state.

Note that in this formulation the differential internal friction state $\delta z(\zeta, t)$, depends on both time t , and space ζ . Indeed, Eq. (2.8) describes a partial differential equation.

$$\frac{d\delta z}{dt}(\zeta, t) = \frac{\partial \delta z}{\partial \zeta}(\zeta, t) + \frac{\partial \delta z}{\partial t}(\zeta, t) = v_r - \frac{\sigma_0 |v_r|}{Lg(v_r)} \delta z$$

2.4 Relation Between Distributed Dynamical Model and the Magic Formula

The linear motion of the differential dF in the patch frame O_p is $\dot{\zeta} = r\omega$, for positive ω , and $\dot{\zeta} = -r\omega$, for negative ω (the frame origin change location when the wheel velocity reverses). Hence $\dot{\zeta} = r|\omega|$. We can thus rewrite (2.8) in the ζ coordinates as

$$\frac{d\delta z}{dt}(\zeta, t) = \frac{d\delta z}{d\zeta} \frac{d\zeta}{dt}(\zeta, t) = \frac{d\delta z}{d\zeta} |r\omega| = v_r - \frac{\sigma_0 |v_r|}{Lg(v_r)} \delta z \quad (2.10)$$

$$\frac{d\delta z}{d\zeta} = -\frac{\sigma_0 |s|}{Lg(v_r)} \delta z + s \operatorname{sgn}(r\omega - v). \quad (2.11)$$

Assuming that v , and ω are constant (hence also v_r , and s), the above equation describes a linear space invariant system having the sign of the relative velocity as its input.

Considering a positive value for $\text{sgn}(r\omega - v)$ over the space interval $[\zeta(t_0), \zeta(t_1)]$, or equivalent over $[\zeta_0, \zeta_1]$, we have that the solution of the above equation is:

$$\delta z(\zeta_1) = \delta z(\zeta_0) e^{-\frac{\sigma_0 |s|}{Lg(v_r)}(\zeta_1 - \zeta_0)} + \frac{Lg(v_r)}{\sigma_0} \left(1 - e^{-\frac{\sigma_0 |s|}{Lg(v_r)}(\zeta_1 - \zeta_0)}\right)$$

Introducing this solution together with Eq. (2.11) in Eq. (2.9), and integrating with $\delta z(\zeta_0) = \zeta_0 = 0$, we have that $F(s)$, is given as:

For the driving case:

$$F(s, \omega) = F_n g(s) \left[1 - (1 - \sigma_1 s) \frac{g(s)}{\sigma_0 s} \left(e^{-\frac{\sigma_0 s}{g(s)}} - 1\right)\right] + \sigma_2 r \omega s \quad (2.12)$$

with

$$g(s) = \mu_C + (\mu_S - \mu_C) e^{-|r\omega s/v_s|^{1/2}}$$

for some constant ω , and $s \in [0, 1]$.

For the breaking case:

$$F(s, v) = F_n g(s) \left[1 - (1 - \sigma_1 s) \frac{g(s)}{\sigma_0 s} \left(e^{-\frac{\sigma_0 v}{g(s)}} - 1\right)\right] + \sigma_2 v s \quad (2.13)$$

with

$$g(s) = \mu_C + (\mu_S - \mu_C) e^{-|v s/v_s|^{1/2}}$$

for some constant v , and $s \in [0, 1]$.

Figure 3 shows the plot of $F(s)$ with the parameters shown in the table 2.1.

Parameter	Value	Unit
σ_0	40	[N/m]
σ_1	4.9487	[N · s/m]
σ_2	0.0018	[N · s/m]
μ_C	0.5	[-]
μ_S	0.9	[-]
v_s	12.5	[m/s]

TABLE 2.1. Data used for the plot shown in Fig. 3 and Fig. 4

Uncertainty in the knowledge of the function $g(v_r)$, can be modeled by introducing the parameter θ , as

$$g(v_r) = \frac{\tilde{g}(v_r)}{\theta},$$

where $\tilde{g}(v_r)$ is some nominal known value for $g(v_r)$. Computation of the function $F(s, \theta)$, from Eq. (2.13), as a function of θ , gives the curves shown

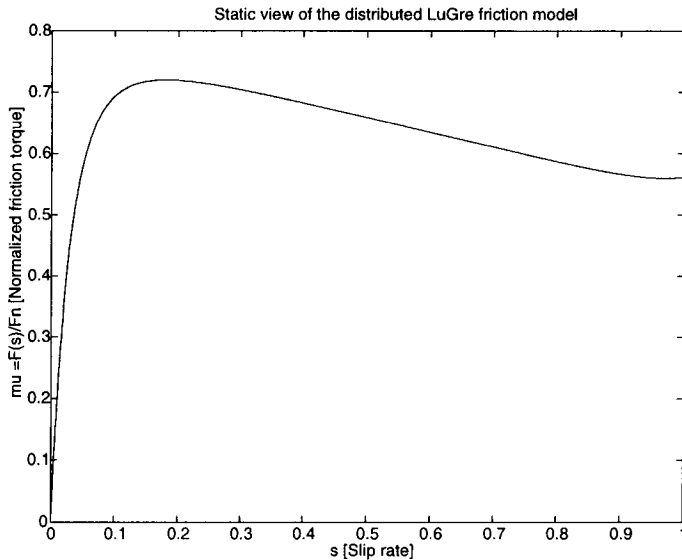


FIGURE 3. Static view of the distributed LuGre model (breaking case, with $v = 20\text{m/s} = 72\text{Km/h}$). This curve shows the normalized friction $\mu = F(s)/F_n$, as a function of the slip rate s .

in Fig. 4. These curves matches reasonable well the experimental data shown in Fig. 1-(a), for different coefficient of road adhesion. Hence, the parameter θ , suitable describes the changes in the road characteristics.

Note that the pseudo-static representation, Eqs. (2.12) and (2.13), does not depends on the patch length L . Hence, the parameters obtained by feeding this model to experimental data, can also be used in the simpler lumped model. This model will be used in the sequel for the observation problem to be defined next.

3 Problem Formulation

We consider the one-wheel model with the lumped tire/road friction model, i.e.

$$m\dot{v} = F_n(\sigma_0 z + \sigma_1 \dot{z}) + F_n \sigma_2 v_r \quad (2.14)$$

$$J\dot{\omega} = -r F_n(\sigma_0 z + \sigma_1 \dot{z}) - \sigma_\omega \omega + u_\tau \quad (2.15)$$

$$\dot{z} = v_r - \theta \frac{\sigma_0 |v_r|}{g(v_r)} z \quad (2.16)$$

with,

$$g(v_r) = \mu_C + (\mu_S - \mu_C) e^{-|v_r/v_s|^{1/2}},$$

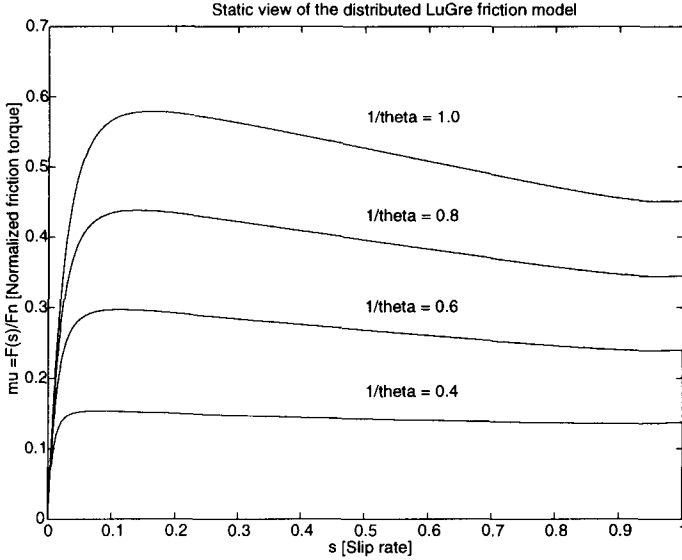


FIGURE 4. Static view of the distributed LuGre model, under different values for $1/\theta$. Breaking case, with $v = 20\text{m/s} = 72\text{Km/h}$. This curve shows the normalized friction $\mu = F(s)/F_n$, as a function of the slip rate s .

where we have neglected the term σ_2 in the equation (2.15), and introduced the parameter θ to capture variation and uncertainties in the function $g(v_r)$. The observation problem can be now formulated as follows.

Problem formulation: Assume that the lumped friction parameters with $\theta = 1$, has been identified off-line, and assume that the variable ω , and v are measurable from some sensors (the need for the measure of v may be relaxed later). The problem is to design an on-line observer for θ , that allows the controller to monitor the eventual changes in the road conditions.

4 General Observer Design

Consider the following system:

$$\dot{x} = Ax + B[\theta\varphi(y, u, x)] + Ru + Ey \quad (2.17)$$

$$\dot{\theta} = 0 \quad (2.18)$$

$$y = C^T x \quad (2.19)$$

with $y, \theta, \varphi(y, u, x) \in R, x \in R^n$, and $u \in R^m$.

We assume that system states are bounded, and that the following holds:

A1) (A, C) is an observable pair,

A2) One of the following properties holds for $\varphi(y, u, x)$:

There exist a known function $\infty > \rho_0 \geq \rho(y, u) \geq 0$, such that:

$$\begin{aligned} (i) \quad & |\varphi(y, u, x_1) - \varphi(y, u, x_2)| \leq \rho(y, u) \|x_1 - x_2\|, \quad \forall x_1, x_2, \\ (ii) \quad & |\varphi(y, u, x)| \leq \rho(y, u) \|x\|, \quad \forall x, \end{aligned}$$

A3) The map $\psi \mapsto \tilde{y}$ of the system

$$\dot{\tilde{x}} = [A - KC^T]\tilde{x} + B\psi \quad (2.20)$$

$$\tilde{y} = C^T \tilde{x} \quad (2.21)$$

is strictly passive, i.e. $\forall Q > 0, \exists P = P^T > 0$, and K , such that

$$P[A - KC^T] + [A - KC^T]^T P = -Q \quad (2.22)$$

$$PB = C. \quad (2.23)$$

A4) The trajectories of the system $(y(t), u(t), x(t))$, satisfy:

$$\lim_{t \rightarrow \infty} \varphi(y(t), u(t), x(t)) \neq 0$$

Under this hypothesis, we propose the following observer structure:

$$\dot{\hat{x}} = A\hat{x} + B \left[\hat{\theta} \varphi(y, u, \hat{x}) \right] + Ru + Ey + K(y - \hat{y}) + B\nu_1 \quad (2.24)$$

$$\dot{\hat{\theta}} = \nu_2 \quad (2.25)$$

$$\hat{y} = C^T \hat{x} \quad (2.26)$$

where ν_1 , and ν_2 , are design variables, which will be defined subsequently.

Introducing the error variables:

$$\tilde{x} = x - \hat{x} \quad (2.27)$$

$$\tilde{\theta} = \theta - \hat{\theta} \quad (2.28)$$

$$\tilde{y} = y - \hat{y} = C^T \tilde{x}, \quad (2.29)$$

The error equation becomes

$$\dot{\tilde{x}} = [A - KC^T]\tilde{x} + B \left[\theta \varphi(y, u, x) - \hat{\theta} \varphi(y, u, \hat{x}) \right] - B\nu_1 \quad (2.30)$$

$$\dot{\tilde{\theta}} = -\nu_2 \quad (2.31)$$

$$\tilde{y} = C^T \tilde{x}, \quad (2.32)$$

where,

$$\theta \varphi(y, u, x) - \hat{\theta} \varphi(y, u, \hat{x}) = \tilde{\theta} \varphi(y, u, \hat{x}) + \theta [\varphi(y, u, x) - \varphi(y, u, \hat{x})]$$

Now, defining the Lyapunov function

$$V = \tilde{x}^T P \tilde{x} + \frac{1}{\gamma} \tilde{\theta}^2$$

and using properties A1, and A3, we have

$$\dot{V} = -\tilde{x}^T Q \tilde{x} + 2\tilde{\theta} [\tilde{y}\varphi(y, u, \hat{x}) - \gamma^{-1}\nu_2] \quad (2.33)$$

$$+ 2\tilde{y}\theta [\varphi(y, u, x) - \varphi(y, u, \hat{x})] - \tilde{y}\nu_1 \quad (2.34)$$

Defining the adaptation law ν_2 as

$$\nu_2 = \gamma\varphi(y, u, \hat{x})\tilde{y} \quad (2.35)$$

we obtain

$$\dot{V} \leq -\tilde{x}^T Q \tilde{x} + 2|\tilde{y}||\theta| [\varphi(y, u, x) - \varphi(y, u, \hat{x})] - \tilde{y}\nu_1. \quad (2.36)$$

If A2 – (i) holds, then we have,

$$\dot{V} \leq -\tilde{x}^T Q \tilde{x} + 2|\tilde{y}||\theta|\rho(y, u)\|\tilde{x}\| - \tilde{y}\nu_1 \quad (2.37)$$

$$\leq -q\|\tilde{x}\|^2 + 2\|C^T\|\|\theta\|\rho(y, u)\|\tilde{x}\|^2 - \tilde{y}\nu_1 \quad (2.38)$$

$$\leq -\|\tilde{x}\|^2(q - 2\|C^T\|\|\theta\|\rho_0) - \tilde{y}\nu_1, \quad (2.39)$$

where

$$q = \lambda_{\min} Q.$$

Since (2.22) holds for any Q , the minimum eigenvalue of Q can be selected such that the term within the parenthesis of the last inequality is positive, i.e.

$$q = 2\|C^T\|\|\theta\|\rho_0 + q_0$$

with any $q_0 > 0$, and $\theta_{max} \geq |\theta|$. Note that a value of θ_{max} can be obtained from the knowledge on the road characteristics, as discussed in previous sections.

In this case we can simply set $\nu_1 = 0$, to get

$$\dot{V} \leq -q_0\|\tilde{x}\|^2.$$

In the second case, when only A2 – (ii) holds, we have

$$\dot{V} \leq -\tilde{x}^T Q \tilde{x} + 2|\tilde{y}||\theta|\rho(y, u)(\|x\| - \|\hat{x}\|) - \tilde{y}\nu_1 \quad (2.40)$$

$$\leq -\tilde{x}^T Q \tilde{x} - |\tilde{y}|[-2\theta_{max}\rho(y, u)(\|x\|_{max} - \|\hat{x}\|) + \text{sgn}(\tilde{y})\nu_1] \quad (2.41)$$

which suggests that ν_1 should be defined to have a high-gain component, i.e.

$$\nu_1 = 2\theta_{max}\rho(y, u)(\|x\|_{max} - \|\hat{x}\|)\text{sgn}(\tilde{y}),$$

where θ_{max} , and $\|x\|_{max}$, are respectively constant upper bounds of the parameter θ and the state norm $\|x\|$.

With this choice of ν_1 we have as before that

$$\dot{V} \leq -q\|\tilde{x}\|^2.$$

Thus, in both of the cases considered by assumption A2 \tilde{x} , and $\tilde{\theta}$ are bounded, and $\tilde{x} \rightarrow 0$. Finally, from the error equation (2.30), we have that

$$\lim_{t \rightarrow \infty} \left\{ B\tilde{\theta}\varphi(y, u, x) \right\} = 0,$$

which together with assumption A4 leads us to conclude that

$$\lim_{t \rightarrow \infty} \hat{\theta} = \theta.$$

We have proved the following theorem:

Theorem 2.1 *Consider the following system*

$$\dot{x} = Ax + B[\theta\varphi(y, u, x)] + Ru + Ey \quad (2.42)$$

$$\dot{\theta} = 0 \quad (2.43)$$

$$y = C^T x \quad (2.44)$$

under the assumptions A1 – A4, with $y, \theta, \varphi(y, u, x) \in R$, $x \in R^n$, and $u \in R^m$. Then the following observer

$$\dot{\hat{x}} = A\hat{x} + B \left[\hat{\theta}\varphi(y, u, \hat{x}) \right] + Ru + Ey + K(y - \hat{y}) + B\nu_1 \quad (2.45)$$

$$\dot{\hat{\theta}} = \gamma\varphi(y, u, \hat{x})\tilde{y} \quad (2.46)$$

$$\hat{y} = C^T \hat{x}, \quad (2.47)$$

with

$$\nu_1 = \begin{cases} 0 & \text{if A2-(i) holds} \\ 2\theta_{max}\rho(y, u)(\|x\|_{max} - \|\hat{x}\|)\text{sgn}(\tilde{y}) & \text{if A2-(ii) holds} \end{cases} \quad (2.48)$$

ensures (under verification of A4), that

$$\lim_{t \rightarrow \infty} \hat{\theta} = \theta.$$

5 Application to the One-Wheel Model

We consider the one-wheel model with lumped friction as described by the equations (2.14)-(2.16). As formulated previously, we assume that both v

and ω are measurable variables. To set our system in the same framework that the structure (2.17)-(2.19), we introduce the new variable

$$\chi = J\omega + rF_n\sigma_1 z,$$

from which we get:

$$\dot{\chi} = -\frac{\sigma_0}{\sigma_1}\chi + (J\frac{\sigma_0}{\sigma_1} - \sigma_\omega)\omega + u_\tau \quad (2.49)$$

$$\dot{z} = (r\omega - v) - \theta\sigma_0\frac{|r\omega - v|}{g(v_r)}z \quad (2.50)$$

$$y = \frac{1}{J}(\chi - rF_n\sigma_1 z) = \omega. \quad (2.51)$$

Defining x , u and y respectively as

$$x = \begin{bmatrix} \chi \\ z \end{bmatrix}, \quad u = \begin{bmatrix} u_\tau \\ v \end{bmatrix}, \quad y = \omega,$$

we can rewrite the above system as

$$\dot{x} = \begin{bmatrix} -\frac{\sigma_0}{\sigma_1} & 0 \\ 0 & 0 \end{bmatrix} x + \begin{bmatrix} 0 \\ 1 \end{bmatrix} \theta\varphi(y, u, x) + \begin{bmatrix} (J\frac{\sigma_0}{\sigma_1} - \sigma_\omega) \\ r \end{bmatrix} y + \begin{bmatrix} 1 & 0 \\ 0 & -1 \end{bmatrix} \begin{bmatrix} u_\tau \\ v \end{bmatrix}$$

where $\varphi(y, u, x)$, is defined as

$$\varphi(y, u, x) = -\frac{\sigma_0|ry - v|}{g(ry - v)}z.$$

With this representation we shall now verify condition under which the assumptions A1 – A3 hold. The last condition A4 depends on the operational conditions, in particular on the applied torque u_τ .

Condition A1 (linear observability). With A , and C defined as above, i.e

$$A = \begin{bmatrix} -\frac{\sigma_0}{\sigma_1} & 0 \\ 0 & 0 \end{bmatrix} \quad C = \begin{bmatrix} \frac{1}{J} \\ -rF_n\sigma_1 \end{bmatrix}$$

we have that condition A1 holds for any values of the system parameters.

$$\text{rank}[C, A^T C] = \text{rank} \begin{bmatrix} \frac{1}{J} & 0 \\ -rF_n\sigma_1 & rF_n\sigma_0 \end{bmatrix} = 2$$

This rank condition clearly shows that the existence a non-zero normal force F_n is necessary to build the friction observer.

Condition A2 (global Lipschitz condition). With $\varphi(y, u, x) = -\frac{\sigma_0|ry-v|}{g(ry-v)}z$, we have that

$$|\varphi(y, u, x_1) - \varphi(y, u, x_2)| \leq \frac{\sigma_0|ry-v|}{g(ry-v)}|z_1 - z_2| \leq \rho(y, u)|z_1 - z_2| \leq \rho(y, u)\|x_1 - x_2\|$$

where $\rho(y, u) = \sigma_0 \mu_C |ry - v|$.

Condition A3 (Passivity). Finding a vector K , so that the map $\psi \mapsto \tilde{y}$ of the system description (2.20)-(2.21), is strictly passive, is equivalent to searching for a vector $K = [k_1, k_2]^T$, such that the I/O-map $G(s)$, defined as

$$G(s) = C^T [Is - A + KC^T]^{-1} B, \quad (2.52)$$

is strictly positive real (SPR), i.e. $\text{Re}\{G(j\omega)\} > 0, \forall \omega \in [0, \infty]$

Computation of $G(s)$ with the corresponding values for A, B, C gives the map

$$G(s) = \frac{s + \beta}{s^2 + \alpha_1 s + \alpha_2} \quad (2.53)$$

with

$$\begin{aligned} \beta &= \frac{\sigma_0}{\sigma_1} + \frac{k_1}{J} \\ \alpha_1 &= \beta - k_2 \frac{rF_n \sigma_1}{J} \\ \alpha_2 &= -\beta k_2 \frac{rF_n \sigma_1}{J} + k_1 k_2 \frac{rF_n \sigma_1}{J^2} \end{aligned}$$

A sufficient condition to this function be SPR is that $k_2 < 0$. Then a simple choice for K is thus

$$\begin{aligned} k_1 &= 0 \\ k_2 &= -k, \end{aligned}$$

for some $k > 0$. From the Kalman-Yakubovich-Popov lemma, we thus ensure with this choice of K that there exist P satisfying the Lyapunov equation with $PB = C$.

Condition A4 (Persistence of excitation). To ensure parameter convergence we need to guarantee that

$$\lim_{t \rightarrow \infty} \varphi(y(t), u(t), x(t)) = \lim_{t \rightarrow \infty} \frac{\sigma_0 |ry(t) - v(t)|}{g(ry - v)} z(t) \neq 0.$$

This implies that the relative velocity should not tend to zero in order for the estimated parameter to converge. This in turn implies that the internal friction state $z(t)$ will not asymptotically converge to zero.

Finally, we have,

Theorem 2.2 Consider the one-wheel model with lumped dynamic friction (2.49)-(2.51), then the following observer:

$$\dot{\hat{\chi}} = -\frac{\sigma_0}{\sigma_1}\hat{\chi} + (J\frac{\sigma_0}{\sigma_1} - \sigma_\omega)\omega + u_\tau \quad (2.54)$$

$$\dot{\hat{z}} = (r\omega - v) - \hat{\theta}\frac{\sigma_0|r\omega - v|}{g(v_r)}\hat{z} - k(\omega - \hat{y}) \quad (2.55)$$

$$\dot{\hat{\theta}} = -\gamma\frac{\sigma_0|r\omega - v|}{g(v_r)}\hat{z}(\omega - \hat{y}) \quad (2.56)$$

$$\hat{y} = \frac{1}{J}(\hat{\chi} - rF_n\sigma_1\hat{z}), \quad (2.57)$$

with positive nonzero k , and γ , ensures that all the estimated states are bounded, and that:

$$\lim_{t \rightarrow \infty} \hat{\chi} = \chi \quad (2.58)$$

$$\lim_{t \rightarrow \infty} \hat{z} = z. \quad (2.59)$$

If in addition, the relative contact velocity does not vanishes, then we also have that

$$\lim_{t \rightarrow \infty} \hat{\theta} = \theta.$$

5.1 Simulation Results

Simulations have been performed with the one-wheel system and the lumped LuGre model. The friction parameters used in the simulations are the ones given in Table 1, with the following additional values for the wheel: $r = 25[cm]$, $m = 5[Kg]$, $J = 0.75 * m * r^2 = 0.2344[Kgm^2]$, $F_n = 14[Kgm^2/s^2]$.

Fig. 5, shows simulation results. Fig. 5-(a) shows the time-profile of the contact friction force resulting from the application of the time torque profile $u_\tau(t)$ shown in Fig. 5-(c). The simulation has first an acceleration phase, and then a breaking phase. From Fig. 5-(a), we can see that about 2 seconds are needed for the friction torque to reach its maximum value.

The observation error of the χ , and z is shown in Fig. 5-(d). According to the theorem these two variables should converge to their true values regardless the profile evolution of the system states. This is verified by this curve showing the exponential convergence of the $\|(\tilde{\chi}(t), \tilde{z})\|$ to zero.

Since the ultimate goal of this work is to be able to on-line estimate this variation, the simulation was done under variations of the parameter θ , representing the road variation conditions (see Fig. 4). Fig. 5-(b) shows in bold lines the value of θ , which evolves within fourth different conditions: the first quarter of the simulation corresponds to dry asphalt conditions. The second quarter corresponds to a sudden change from dry to wet. During the third quarter, there is a smooth variation from wet to snow. The last

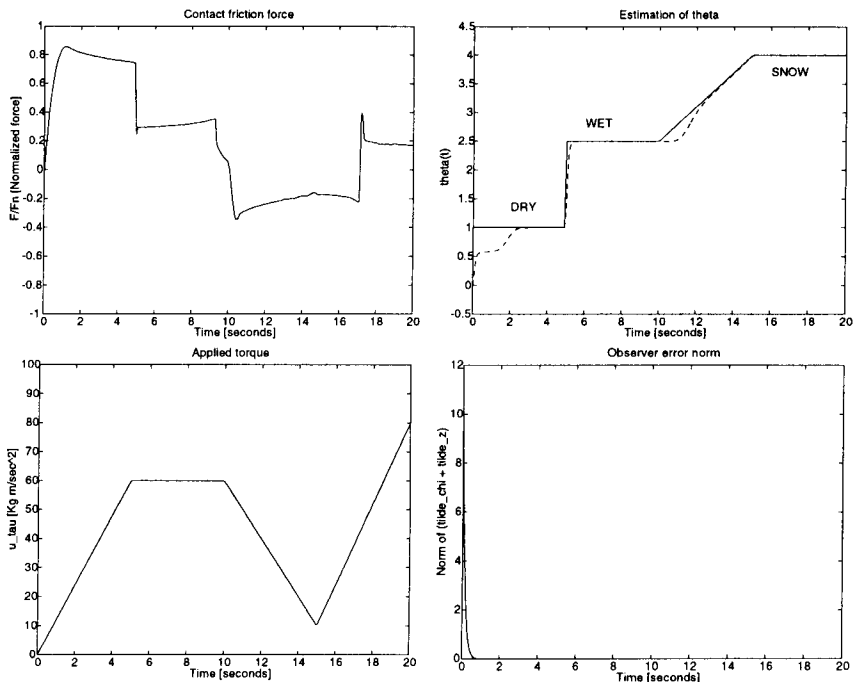


FIGURE 5. a) Contact torque friction $F(t)$ (up left). b) Estimated parameter $\hat{\theta}(t)$, and evolution of θ (up right). c) Applied wheel torque $u_{\tau}(t)$ (low left). d) Observer error norm of $(\tilde{x}(t), \tilde{z})$ (low right).

quarter is kept constant at the snow conditions. In dotted lines we can see the evolution of the estimate $\hat{\theta}(t)$. As we can observe, a good parameter tracking is obtained, as long as the relative contact velocity is different from zero. During the small time-period when this velocity is small or zero, the adaptation law yields a constant $\hat{\theta}(t)$.

6 Conclusions

We have presented a method to estimate on-line the changes in road condition. To achieve this goal we have introduced dynamical friction models that, on one hand, provide a more accurate description of the contact friction, and on the other hand, allow us to characterize road condition variations via a single parameter.

It has been shown that the distributed parameter version of these models also captures stationary shape profiles between normalized friction and slip rate that are similar to the ones obtained from experimental data (i.e. magic formula).

We have introduced a model-base observer that ensure asymptotic tracking of road condition, under mild conditions implying a non-vanishing evolution of the slip rate. This condition are quite natural in this context (they imply that the vehicle should operate away to the ideal pure rolling condition). Mathematically, this condition correspond to the persistently excitation condition, which is well known in the adaptive control literature. In the context of nonlinear observers, this condition appear as being the characterization of “good ” inputs, which are required to recover state observability.

The observer presented here has been derived in a general framework allowing to extend our study to the case where the vehicle velocity is not measurable. In particular, assumption $A2 - (ii)$ will allows for this extension, if it can be shown that the assumption $A3$, also holds. This study and the introduction of other factors like: wheel vertical deformation, and suspension dynamics, are currently under study.

Acknowledgements

The LuGre version of the dynamic friction model presented here, was derived during the first author visit at the Department of Aeronautics at the Georgia Institute of Technology (CNRS/NSF collaboration project). A more complete report on this topic is in preparation.

The first author would like also to thanks M. Sorin and P.A. Bliman for the interesting discussion on distributed friction models.

7 REFERENCES

- [1] E. Bakker, L. Nyborg and H. Pacejka. Tyre Modelling for Use in Vehicle Dynamic Studies. Society of Automotive Engineers Paper # 870421, 1987.
- [2] P. A. Bliman, T. Bonald and M. Sorine. Hysteresis Operators and tire Friction Models: Application to vehicle dynamic Simulator. *Prof. of ICIAM. 95*, Hamburg, Germany, 3-7 July, 1995.
- [3] M. Burckhardt. ABS und ASR, Sicherheitsrelevantes, Radschlupf-Regel System, *Lecture Scriptum*. University of Braunschweig, Germany, 1987.
- [4] M. Burckhardt. *Fahrwerktechnik: Radschlupfregelsysteme*. Vogel-Verlag, Germany, 1993.
- [5] C. Canudas de Wit, H. Olsson, K. J. Åström and P. Lischinsky. A New Model for Control of Systems with Friction, *IEEE TAC*, Vol. 40, No. 3, pp.419-425, March 1995.

- [6] C. Canudas de Wit and P. Lischinsky. Adaptive friction compensation with partially known dynamic friction model, *International Journal of Adaptive Control and Signal Processing*, Vol. 11, pp.65-85, 1997.
- [7] P. R. Dahl. Solid Friction Damping of Mechanical Vibrations. *AIAA Journal*, 14, No. 12, pp.1675-1682, 1997.
- [8] F. Gustafsson. Slip-based Tire-road Friction Estimation. *Automatica*, 33(6):1087-1099, 1997.
- [9] J. Harned, L. Johnston and G. Scharpf. Measurement of Tire Brake Force Characteristics as Related to Wheel Slip (Antilock) Control System Design. *SAE Transactions*, 78(690214):909-25, 1969.
- [10] U. Kiencke. Realtime Estimation of Adhesion Characteristic Between Tyres and Road. In *Proceedings of the IFAC World Congress*, volume 1, 1993.
- [11] U. Kiencke and A. Daiss. Estimation of Tyre Friction for Enhanced ABS-Systems. In *Proceedings of the AVEG'94*, 1994.
- [12] H. Lee and M. Tomizuka. Adaptive Traction Control. PATH Technical Report UCB-ITS-PRR-95-32, Institute of Transportation Studies, University of California at Berkeley, 1995.
- [13] Y. Liu and J. Sun. Target Slip Tracking Using Gain-Scheduling for Antilock Braking Systems. In *The American Control Conference*, pages 1178-82, Seattle, Washington, 1995.
- [14] H. B. Pacejka and R. S. Sharp. Shear Force Developments by Pneumatic tires in Steady-state conditions: A review of Modeling Aspects.. *Vehicle Systems Dynamics*, Vol. 20, pp.121-176, 1991.
- [15] W. R. Pasterkamp and H. B. Pacejka. The Tire as a Sensor to Estimate Friction. *Vehicle Systems Dynamics*, Vol. 29,(1997) pp.409-422, 1997.
- [16] L. R. Ray. Nonlinear Tire Force Estimation and Road Friction Identification: Simulation and Experiments. *Automatica*, 33(10):1819-1833, 1997.
- [17] H. T. Szostak, R. W. Allen and T. J. Rosenthal. Analytical Modeling of Driver Response in Crash Avoidance Maneuvering. Volume II: An Interactive Tire Model for Driver/Vehicle Simulation. Report no. DOT HS 807-271, U.S. Department of Transportation, 1988.
- [18] K. Yi and T. Jeong. Observer Based Estimation of Tire-road Friction for Collision Warning Algorithm Adaptation. *JSME International Journal*, 41(1):116-124, 1998.